Advanced Signal Processing Techniques Applied to Terahertz Inspections on Aerospace Foams

Long Buu Trinh

Lockheed Martin Space Systems Company, Technology Laboratories, 11380 Old Gentilly Rd., New Orleans, LA 70129

References and links

1. Zimdars, D., "Fiber-pigtailed terahertz time domain spectroscopy instrumentation for package inspection and security imaging" in Proc. SPIE, **5070**, 108 (2003).
2. Oppenhiem, A.V., and R.W. Schafer, *Discrete-Time Signal Processing*, (Prentice-Hall, 1989).

Abstract: The space shuttle's external fuel tank is thermally insulated by the closed cell foams. However, natural voids composed of air and trapped gas are found as by-products when the foams are cured. Detection of foam voids and foam de-bonding is a formidable task owing to the small index of refraction contrast between foam and air (1.04:1). In the presence of a denser binding matrix agent that bonds two different foam materials, time-differentiation of filtered terahertz signals can be employed to magnify information prior to the main substrate reflections. In the absence of a matrix binder, de-convolution of the filtered time differential terahertz signals is performed to reduce the masking effects of antenna ringing. The goal is simply to increase probability of void detection through image enhancement and to determine the depth of the void.

1.0 Introduction

Terahertz Differentiation Technique

Far-infrared, non-ionizing radiation at a frequency below one terahertz is utilized for the non-destructive evaluation (NDE) on the space shuttle's external fuel tank foam insulation using the Picometrix QA-1000 pulsed terahertz reflection system [1]. The fiber-pigtailed sealed transmitter and receiver are collinearly arranged via a beam splitter. A six inch hyperboloidal polyurethane lens gives an operating focus depth of 11.75 inches at normal incidence. The focus spot size is 0.196 inch or 5 mm. Raster scanning resolution is typically set at 0.06 inch or 1.5 mm for foam NDE. The QA-1000 terahertz system scans a waveform of time duration of 320 picoseconds (ps) at 100 Hz.

A Blackman window finite impulse response filter was chosen to bandpass from 120 to 180 GHz. Noise floor is encountered after approximately 200 GHz due to infrared radiation absorption by the foam. The Nyquist frequency is 3.2-THz. A computation of the first derivative with respect to time on the voltage signal is:

$$\frac{dV(t)}{dt}\Big|_{\Delta t=0.1756\,ps} \qquad (1)$$

where V is the band filtered voltage waveform, t is time, and dt is the 0.1756-ps time-step measurement resolution.

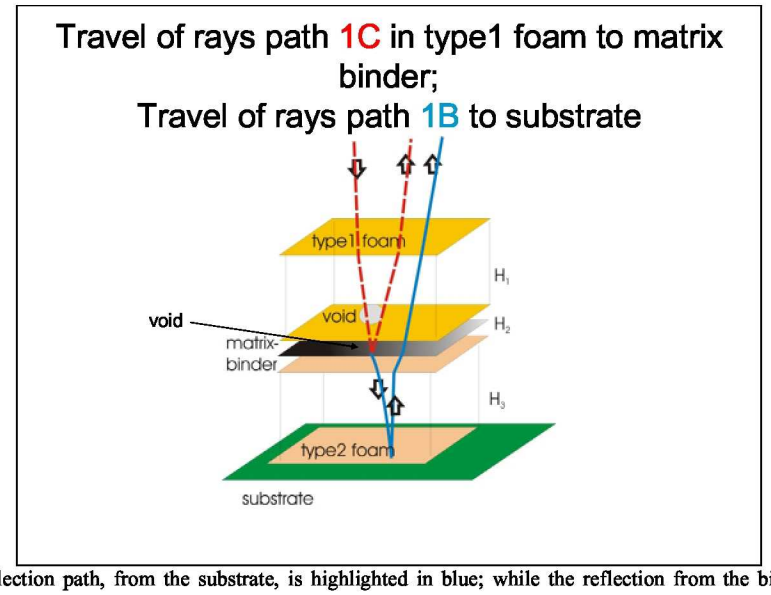

Fig. 1. The main reflection path, from the substrate, is highlighted in blue; while the reflection from the binding matrix agent is highlighted in red.

Figure 1 illustrates the infrared radiation (ir) reflection paths off the metallic substrate (shown in blue) and the partial reflection off the matrix binder interface sandwiched between the foam layers (shown in red). The time derivative method is used to magnify the direct path associated with the partial reflection off of the relatively denser matrix binding agent. The height of the void above the substrate can be estimated by equation 2:

$$(h + H_2 + H_3) \cong \frac{t_{1B} - t_{1C}}{2\alpha}, \qquad (2)$$

where t_{1B} is twtt (ps) associated with the substrate reflection, t_{1C} is twtt (ps) associated with the matrix binder reflection, h is the void thickness (in.), H_2 is the thickness of the matrix binding layer (in.), H_3 is the thickness of the bottom foam layer (in.), and α is the time-distance calibration factor of 51.5 ps/inch.

Figure 2a illustrates the pre-pulse information hidden within the oscillating wave which is revealed by applying the band pass time derivative as shown in figure 2b. The pre-pulse wave segment is magnified by a scaling multiplication factor of 10 for improved visual acuity as well as C-scan enhancement. The Blackman window facilitates the combination of the pre-pulse and post-pulse segments of the waveform. Notice that ringing is observed within the post-pulse data segment.

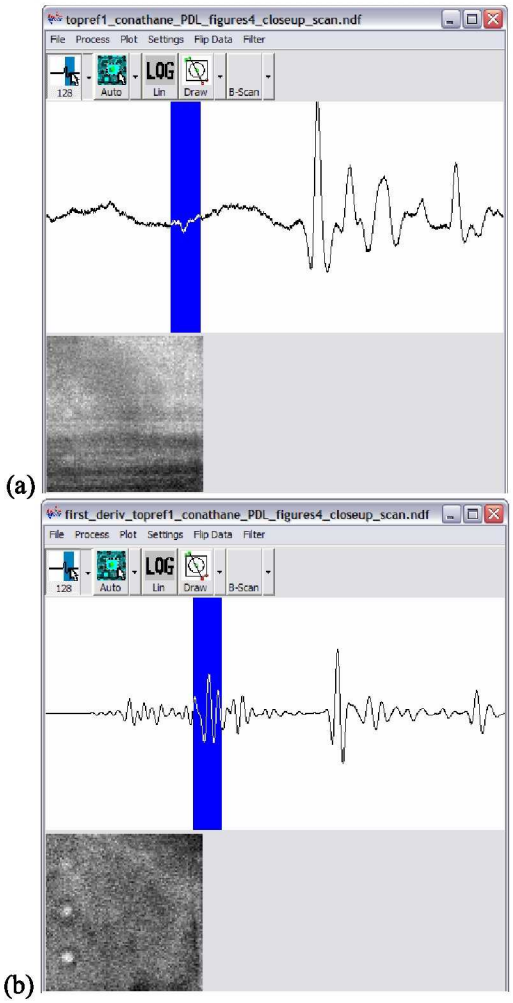

Fig. 2. Peak-peak waveform and C-scan image comparison: (a) raw wave, (b) time derivative filtered wave.

Terahertz De-convolution Technique

In the absence of an applied matrix binding agent layer, foam defects such as voids and incidents of de-bonding can exist at the point of physical contact between the poured and sprayed foam layers. In order to determine the time of flight associated with these subtle features, the masking effects of the substrate and the underlying sprayed foam layer must be minimized.

Figure 3 illustrates a time derivative terahertz waveform from a reference sample and an ideal time derivative pulse utilized in the de-convolution process: note the absence of ringing at the pre-pulse and post-pulse waveform segments.

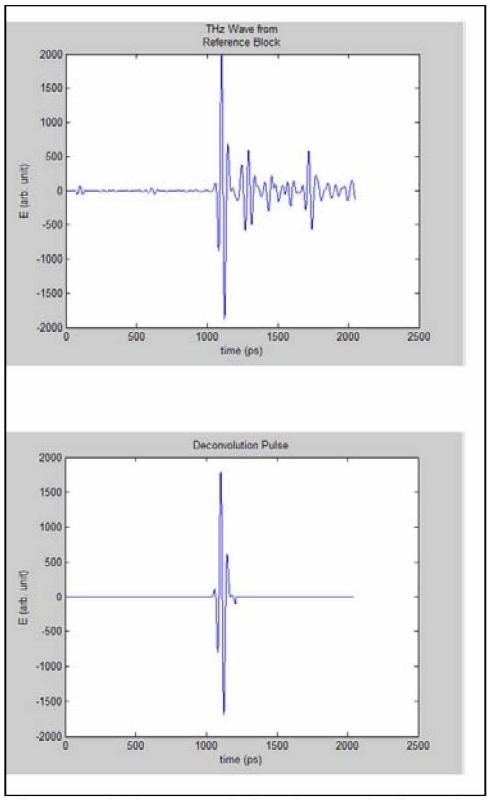

Figure 3. Ideal De-convolution Time-Derivative Pulse.

The de-convolution computation is performed as follows in equation 3:

$$y(t)_{deconv} = F^{-1}\left\{\frac{Y(\omega)_{acq}}{\left(Y(\omega)_{ref}/2X(\omega)_{ideal}\right)}\right\} \quad (3)$$

where $F^{-1} \equiv$ inverse Fourier transform, $Y(\omega)_{acq} \equiv$ spectra of acquired data, $Y(\omega)_{ref} \equiv$ spectrum of reference wave, $X(\omega)_{ideal} \equiv$ spectrum of ideal pulse, $y(t)_{deconv} \equiv$ de-convoluted time pulses, and $\omega \equiv$ frequency.

Figure 4 illustrates the first and second substrate reflecting paths. To estimate the height of the void above the substrate, the difference in the time of flight (ΔT) between the two paths is measured. ΔT is defined in equation 4. Note that equation 4 is equivalent to equation 2 if the matrix binding layer thickness is much thinner than the foam thicknesses.

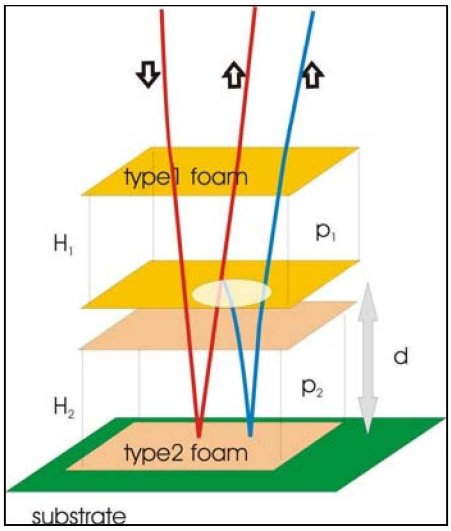

Figure 4. The reflection path from the substrate is highlighted in red, while a second subsequent substrate reflection is highlighted in blue.

$$\Delta T = \left[\frac{2d}{V_2} + \frac{2(H_1 + H_2)}{\sqrt{(V_1 V_2)}}\right] - \frac{2(H_1 + H_2)}{\sqrt{V_1 V_2}} = 2d\alpha$$

$$2d = \frac{\Delta T}{\alpha} \qquad (4)$$

where

$\alpha = 51.5\, ps / inch$

$d \equiv$ height from the substrate to top of the void

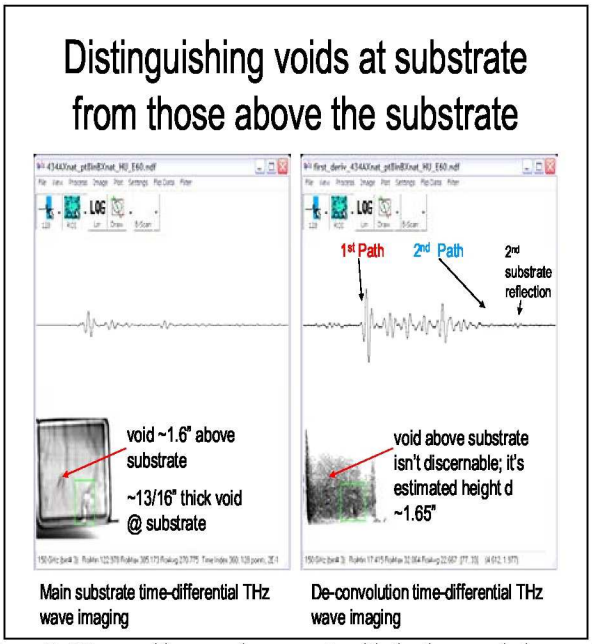

Figure 5. Wave and image enhancements with the de-convolution result.

The presence of a pseudo-natural defect embedded in the upper type 1 foam layer and a natural defect embedded in the lower type 2 foam layer are highlighted in the C-scan image of figure 5 at the main reflecting path. Note that the defect 1.6 inches above the substrate disappears at the indicated time bins prior to the 2nd substrate reflection in the de-convolution image to the right. The time difference between the highlighted paths of interest can be used to compute for the height of the void above the substrate.

Another test case is presented with pseudo-natural voids embedded within the mock-up ice frost ramp (IFR) panel. The voids are embedded in the thicker portion of the IFR at approximately 2.5 inches above the substrate. Figure 6 compares the advantage of the de-convolution technique.

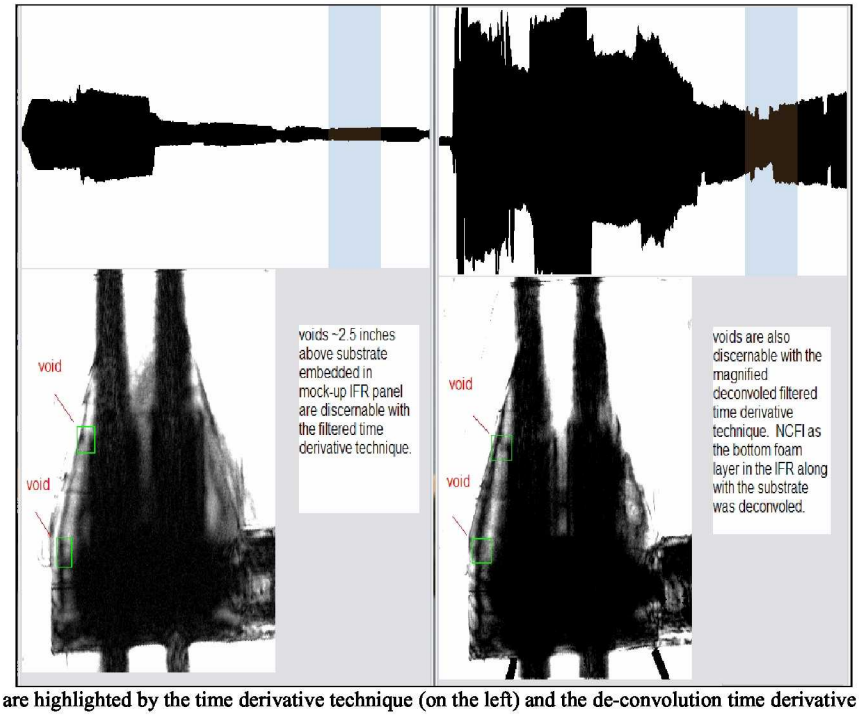

Figure 6. Voids are highlighted by the time derivative technique (on the left) and the de-convolution time derivative technique (on the right).

2.0 Data Analyses

Terahertz Result

A mock-up panel, approximately 36 in. x 36 in., used to represent a sectional part of the tank was divided into two developmental zones. In both zones approximately 0.85 inch of sprayed type 2 foam was first applied to the panel. One zone consisted of the poured type 1 foam layer in contact with the sprayed type 2 foam layer. The other zone consisted of poured type 1 foam layer in contact with the matrix binder, overlying the sprayed type 2 foam layer below. See figures 7.

Figure 6a exhibits de-bonding between the type 1 foam and the type 2 foam layers, while figure 6b exhibits voids found above the matrix binding layer. The height of the void is defined as the distance from the metallic substrate to the top of the void.

For example, the void labeled 8 has a derived, measured height of ≡ base foam thickness + void's thickness,
0.85 inch of type 2 foam + 0.14 inch of type 2 foam = 1.00 inch above the substrate.

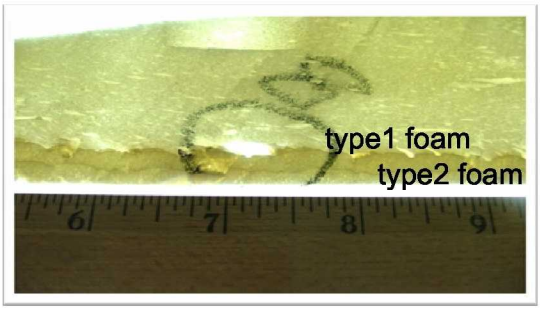

(6a)

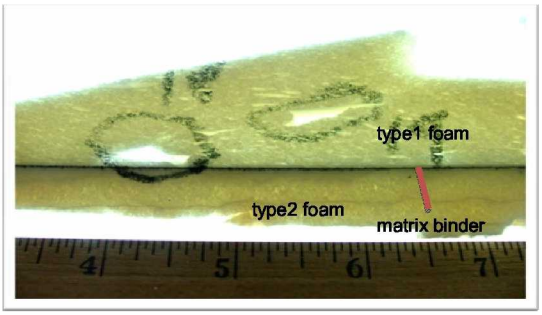

(6b)

Figure 7. (a) De-bonding between separate foam layers in contact. (b) Voids identified in poured foam above the matrix binder and sprayed foam.

Table 1 lists the height estimation results for identified voids in the panel. Estimations were very close to ground truth data where de-bonding exists, as seen in the first half of the table. Overall statistical determination of the height of the foam defect above the substrate was within 10%.

Figure 8 is a distribution plot of the physical dimension of the voids, along with depth estimations.

void #	measured (in.)	estimated (in.)	% difference
2	0.925	0.88	3.0
3	0.938	0.89	2.5
4	1.01	0.97	4.0
5	1.05	0.95	5.3
7	0.99	0.95	2.0
8	1.00	1.02	2.02
9	0.97	0.94	2.08
10	0.96	1.00	0.07
12	0.99	1.02	0.3
14	1.10	0.95	6.7
15	1.01	1.14	-4.4
16	1.02	1.04	-2.5
17	1.00	1.12	-3.9
18	1.05	1.21	-10.4
19	1.45	1.28	2.9
20	1.09	1.00	3.0

Table 1. Comparison between the height of foam void estimation to ground-truth data.

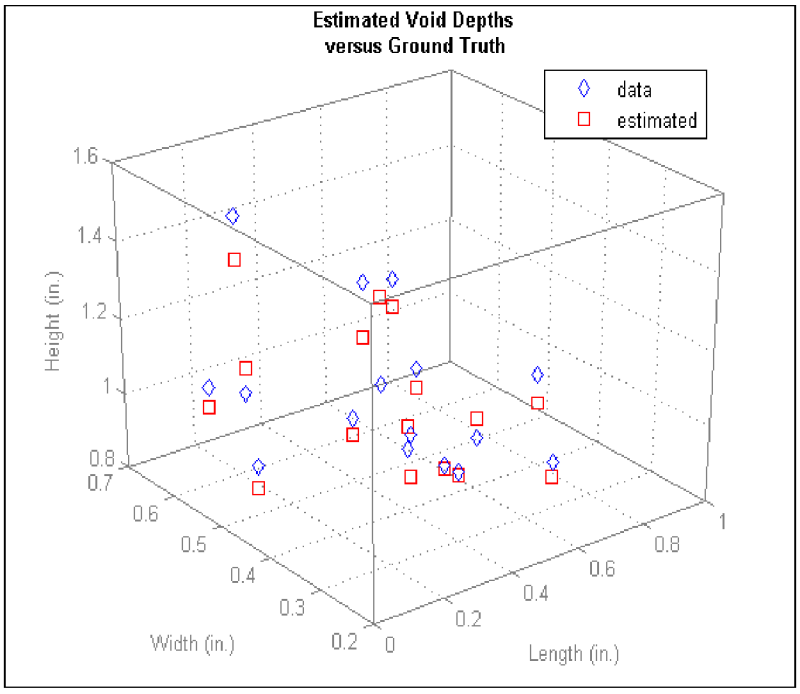

Figure 8. Plot of estimated height of the void versus ground truth data.

3.0 Conclusion

Filtered time-derivative and de-convolution signal processing techniques applied to the pre-pulse and post-pulse segments of the waveforms provided (1) signal magnification, (2) image enhancement, and (3) determination for the height of void above the substrate. A single general formula can be used to compute the height of the defect height with or without the presence of the matrix binding agent.